Inorganic Chemistry

Article

pubs.acs.org/IC

Coordination Chemistry of 4-Methyl-2,6,7-trioxa-1-phosphabicyclo[2,2,1]heptane: Preparation and Characterization of Ru(II) Complexes

Evan E. Joslin, Claire L. McMullin, T. Brent Gunnoe,* Thomas R. Cundari,* Michal Sabat, and William H. Myers

Department of Chemistry, University of Virginia, Charlottesville, Virginia 22904, United States

Center for Advanced Scientific Computing and Modeling (CASCaM), University of North Texas, Denton, Texas 76203, United States

Nanoscale Materials Characterization Facility, Department of Materials Science and Engineering, University of Virginia, Charlottesville, Virginia 22904, United States

Department of Chemistry, University of Richmond, Richmond, Virginia 23173, United States

Supporting Information

ABSTRACT: The complexes TpRu[$P(OCH_2)_2(OCCH_3)$]$(PPh_3)Cl$ (**2**) [Tp = hydridotris(pyrazolyl)borate; $P(OCH_2)_2(OCCH_3)$ (**1**) = (4-methyl-2,6,7-trioxa-1-phosphabicyclo[2,2,1]heptane] and TpRu(L)$(PPh_3)Cl$ [L = $P(OCH_2)_3CEt$ (**3**), PMe_3 (**4**) or $P(OMe)_3$ (**5**)], (η^6-C_6H_6)Ru(L)Cl_2 [L = PPh_3 (**6**), $P(OMe)_3$ (**7**), PMe_3 (**8**), $P(OCH_2)_3CEt$ (**9**), CO (**10**) or $P(OCH_2)_2(OCCH_3)$ (**11**)] and (η^6-*p*-cymene)Ru(L)Cl_2 [L = $P(OCH_2)_3CEt$ (**12**), $P(OCH_2)_2(OCCH_3)P(OCH_2)_2(OCCH_3)$ (**13**), $P(OMe)_3$ (**14**) or PPh_3 (**15**)] have been synthesized, isolated, and characterized by NMR spectroscopy, cyclic voltammetry, mass spectrometry, and, for some complexes, single crystal X-ray diffraction. Data from cyclic voltammetry and solid-state structures have been used to compare the properties of (**1**) with other phosphorus-based ligands as well as carbon monoxide. Data from the solid-state structures of Ru(II) complexes show that $P(OCH_2)_2(OCCH_3)$ has a cone angle of 104 . Cyclic voltammetry data reveal that the Ru(II) complexes bearing $P(OCH_2)_2(OCCH_3)$ have more positive Ru(III/II) redox potentials than analogous complexes with the other phosphorus ligands; however, the Ru(III/II) potential for (η^6-C_6H_6)Ru[$P(OCH_2)_2(OCCH_3)$]Cl_2 is more negative compared to the Ru(III/II) potential for the CO complex (η^6-C_6H_6)Ru(CO)Cl_2. For the Ru(II) complexes studied herein, these data are consistent with the overall donor ability of **1** being less than other common phosphines (e.g., PMe_3 or PPh_3) or phosphites [e.g., $P(OCH_2)_3CEt$ or $P(OMe)_3$] but greater than carbon monoxide.

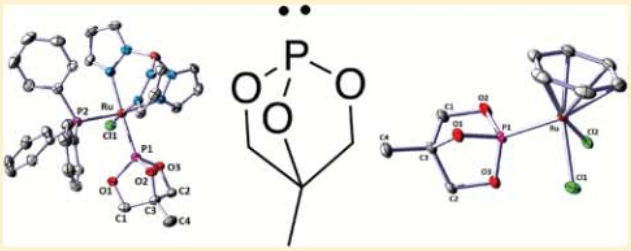

INTRODUCTION

Phosphorus-based compounds offer a wide range of steric properties and basicities because of the variety of accessible substituents.[1 16] In addition, many phosphorus-based compounds bind strongly to transition metals. As a result of their coordinating ability and highly tunable stereoelectronic character, phosphorus-based compounds are among the most heavily utilized class of ligands in coordination chemistry and homogeneous catalysis.[1 3,5 7,9,16 19] Several studies have quantified the steric and donor properties of a wide range of phosphorus-based ligands.[6,8,10 16,20 22] For example, the classic work by Tolman established the comparison of the steric properties of phosphorus ligands using cone angles.[6] Recently, predicting the steric properties of phosphorus-based ligands has been improved using crystallographic data and computer modeling software.[6,14,18] The donor abilities of phosphorus ligands have been studied using CO absorption energies for metal carbonyl complexes with phosphorus ligands [e.g., $Ni(CO)_3L$ where L = phosphite, phosphine, etc.].[6]

Bicyclic phosphites have been investigated and compared to acyclic phosphites. In general, the steric profiles of bicyclic phosphites are constrained relative to acyclic compounds, and bicyclic phosphites exhibit reduced basicity relative to acyclic phosphites. Verkade has proposed the hinge effect to explain the influence of the bicyclic phosphites rigidity on basicity (Scheme 1).[3,23 26] Uncoordinated phosphites adopt a trigonal pyramidal geometry, while coordination (or protonation) of the phosphite results in a shift toward tetrahedral geometry. Upon coordination to a metal center, the O P O and the P O C

Received: January 16, 2012
Published: March 27, 2012

   dx.doi.org/10.1021/ic300109b | Inorg. Chem. 2012, 51, 4791 4801

Scheme 1. Comparison of Acyclic and Bicyclic Phosphites Based on the Hinge Effect

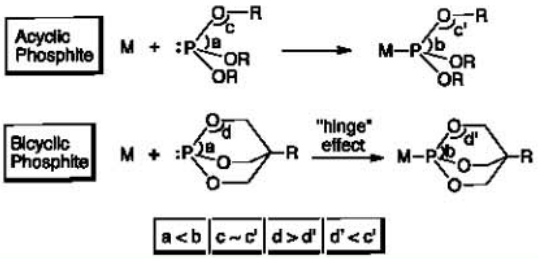

angles of an acyclic phosphite can adjust independently. But, reorganization of bicyclic phosphites upon metal ligation is more restricted because adjustment of the O P O angle influences the P O C angle. For coordinated phosphites, bicyclic phosphites exhibit a smaller P O C angle compared to the acyclic phosphites (i.e., d < c in Scheme 1). Verkade has proposed that these changes result in a reduction of the p-orbital overlap between O and P, which increases the positive charge on the P atom and decreases the basicity relative to acyclic phosphites. Thus, the donor ability of bicyclic phosphites is reduced relative to related acyclic phosphites.[27,28]

A few bicyclic phosphites have been prepared and studied, and similar to acyclic phosphorus-based ligands their steric and donor properties are variable (Chart 1).[6,29] While several

Chart 1. Examples of Bicyclic Phosphites

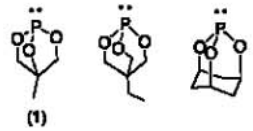

examples of transition metal complexes with bicyclic phosphite ligands are known, including nickel, cobalt, iron, chromium, molybdenum, and tungsten complexes,[2,4,30,32] to our knowledge, no examples of a structurally characterized transition metal complex with $P(OCH_2)_2(OCCH_3)$ (**1**) (4-methyl-2,6,7-trioxa-1-phosphabicyclo[2,2,1]heptane) is known. The structure of the phosphate $O{=}P(OCH_2)_2(OCCH_3)$ has been reported.[29] Verkade et al. have studied a variety of polycyclic phosphorus compounds including their coordination to transition metals.[2,3,24,27,29,30] On the basis of trends in basicity, it is anticipated that **1** would be less donating to metal centers than the more commonly studied bicyclic phosphite $P(OCH_2)_3CEt$.[28]

Phosphorus-based ligands are generally considered good donor ligands; but, the number of weakly donating ligands is small compared to strongly donating P-based ligands. We felt that phosphite **1** might provide a relatively weakly donating phosphorus-based ligand. To study phosphite **1** and compare it to other phosphorus-based ligands, we sought suitable transition metal systems that would allow the coordination of several phosphorus-based ligands. Solid-state structures, redox properties (by cyclic voltammetry), and rates of ligand exchange have been studied for $TpRu(L)(PPh_3)Cl$, $(\eta^6\text{-}C_6H_6)Ru(L)Cl_2$ and $(\eta^6\text{-}p\text{-cymene})Ru(L)Cl_2$ complexes (Chart 2).

RESULTS AND DISCUSSION

The preparation of **1** from 2-methyl-1,2,3-propanetriol has been reported.[33] Our attempts to synthesize and cleanly isolate

Chart 2. $TpRu(L)(PPh_3)Cl$, $(\eta^6\text{-}C_6H_6)Ru(L)Cl_2$ and $(\eta^6\text{-}p\text{-cymene})Ru(L)Cl_2$ Complexes Used to Study the Electronic and Steric Properties of Phosphite 1

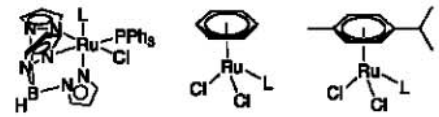

1 using this procedure were not successful. In addition, using alternate procedures reported for similar bicyclic phosphorus species did not result in the clean isolation of **1**.[24,30,34,35] Thus, we developed a modified procedure that involves the in situ generation and subsequent reaction of **1** without isolation.[36,37] The reaction of 2-methyl-1,2,3-propanetriol with NaH followed by treatment with PCl_3 results in clean in situ formation of compound **1**, as evidenced by a single resonance at 115 ppm in the ^{31}P NMR spectrum (eq 1).

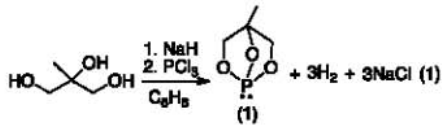

TpRu(L)(PPh$_3$)Cl Complexes. The addition of $TpRu(PPh_3)_2Cl$ to a benzene solution of **1** followed by reflux results in the formation of $TpRu[P(OCH_2)_2(OCCH_3)](PPh_3)Cl$ (**2**) (eq 2).

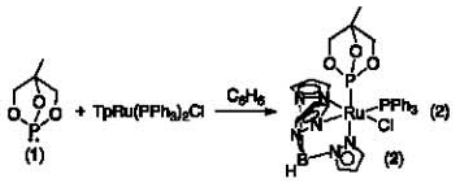

For **2**, the methylene hydrogen atoms are diastereotopic, and the asymmetric complex exhibits four resonances due to the two CH_2 groups with $^2J_{HH}$ = 8 Hz and $^3J_{HP}$ between 8 and 3.6 Hz. In addition, a $^4J_{HH}$ of 1.4 Hz is observed for two of the hydrogen atoms (Table 1).

Table 1. Coupling Constants Observed for the Ligand $P(OCH_2)_2(OCCH_3)$ (1) in the ^1H NMR Spectrum of $TpRu[P(OCH_2)_2(OCCH_3)]PPh_3Cl$

		$^2J_{HH}$	$^3J_{HP}$	$^4J_{HH}$
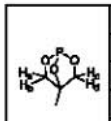	H_a	8.0 Hz	8.0 Hz	-[a]
	H_b	8.0 Hz	3.6 Hz	1.4 Hz
	H_c	8.0 Hz	8.0 Hz	-[a]
	H_d	8.0 Hz	3.6 Hz	1.4 Hz

[a]A third coupling constant was not resolved for these resonances.

An X-ray diffraction study (Table 2) was performed on a crystal of complex **2** (Figure 1). A search of the Cambridge Structural Database revealed no other examples of structures with phosphite **1**. We have previously reported the structure of $TpRu[P(OCH_2)_3CEt](PPh_3)Cl$ (**3**).[31] The Ru $P_{phosphite}$ bond lengths for complexes **2** and **3** are 2.191(1) Å and 2.2025(8) Å, respectively. Thus, phosphite **1** exhibits a slightly shorter Ru $P_{phosphite}$ bond distance than $P(OCH_2)_3CEt$. The average $P_{phosphite}$ O bond distance for complex **2** is 1.627(3) Å, whereas complex **3** has a shorter average $P_{phosphite}$ O bond length of 1.605(2) Å. The longer P O bond distances for **2**

dx.doi.org/10.1021/ic300109b | Inorg. Chem. 2012, 51, 4791 4801

Table 2. Selected Crystallographic Data for TpRu(PPh$_3$)[P(OCH$_2$)$_2$(OCCH$_3$)]Cl (2), (η^6-C$_6$H$_6$)-Ru[P(OCH$_2$)$_2$(OCCH$_3$)]Cl$_2$ (11), and (η^6-*p*-cymene)-Ru[P(OCH$_2$)$_2$(OCCH$_3$)]Cl$_2$ (12)

	complex **2** CH_2Cl_2	complex **11** $(CHCl_3)_2$	complex **12** $(CH_2Cl_2)_2$
empirical formula	$C_{32}H_{34}BCl_3N_6O_3P_2Ru$	$C_{12}H_{15}Cl_8O_3PRu$	$C_{18}H_{29}Cl_6O_3PRu$
fw	830.82	622.88	638.15
cryst syst	monoclinic	monoclinic	monoclinic
space group	$P2_1/c$	$P2_1/c$	$P2_1/n$
a, Å	14.5126(3)	10.219(1)	10.7611(3)
b, Å	13.5883(3)	10.518(1)	10.4473(3)
c, Å	17.8390(4)	20.162(2)	22.4999(6)
β, deg	93.643(1)	99.416(1)	99.312(1)
V, Å^3	3510.8(1)	2137.9(4)	2496.2(1)
Z	4	4	4
D_{calcd}, mg/m^3	1.572	1.935	1.698
cryst size, mm	0.31 0.12 0.07	0.34 0.12 0.11	0.45 0.45 0.14
R1, wR2 ($I > 2\sigma(I)$)	0.0346, 0.0994	0.0492, 0.1298	0.0253, 0.0965
GOF	0.833	1.056	0.863

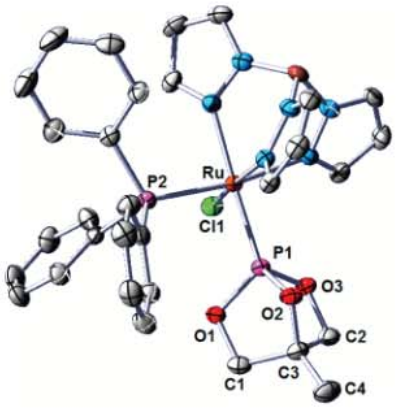

Figure 1. ORTEP of TpRu[P(OCH$_2$)$_2$(OCCH$_3$)](PPh$_3$)Cl (**2**) (50% probability with hydrogen atoms omitted). Selected bond lengths (Å): Ru P1, 2.191(1); Ru P2, 2.342(1); P O1, 1.627(3); P O2, 1.632(3); P O3, 1.620(3). Selected bond angles (deg): P1 Ru P2, 94.1(4); O3 P1 O1, 100.2(1); O3 P1 O2, 94.6(1); O1 P1 O2, 95.0(1); O1 P1 Ru, 118.5(1); O2 P1 Ru, 126.2(1); O3 P1 Ru, 116.8(1); C1 O1 P1, 107.3(2); C3 O2 P1, 97.5(2); C2 O3 P1, 107.4(2).

[compared to P(OCH$_2$)$_3$CEt] are anticipated if ligand **1** functions as a better π-acid than P(OCH$_2$)$_3$CEt and the dπ-backbonding involves the P O σ^* orbitals.[1] Complex **2** exhibits one larger [100.2(1)] and two smaller [94.6(1) and 95.0(1)] O P O bond angles. The O2 P1 Ru angle in complex **2** is 126.2(1) , whereas the O3 P1 Ru and O1 P1 Ru angles are 116.80(1) and 118.49(1) . The O3 $P_{phosphite}$ Ru angles [118.33(9) , 113.34(9) , and 118.79(9)] of **3** are similar to the same angles with O1 and O3 of complex **2**. For the $C_{phosphite}$ O $P_{phosphite}$ angles, complex **2** has one angle smaller than the other two [97.5(2) vs 107.3(2) and 107.4(2)]. For complex **3**, all the angles for $C_{phosphite}$ O $P_{phosphite}$ are similar at 116.9(2) , 115.8(2) , and 116.5(2) . Thus, the $C_{phosphite}$ O $P_{phosphite}$ angles of **2** are smaller than **3**, which is consistent with a more pronounced hinge effect (Scheme 1) for **1** compared to P(OCH$_2$)$_3$CEt. Cone angles were calculated from crystallographic data for the phosphite ligands of complexes **2** and **3**. Using the P1 Ru O angles and the van der Waals radius for oxygen, the cone angle for complex **2** was determined to be 104 , whereas complex **3** is slightly larger at 108 (see Supporting Information).[14] The cone angle of P(OMe)$_3$ is 107 .[6]

In addition to **2** and **3**, we prepared TpRu(PMe$_3$)(PPh$_3$)Cl (**4**) and TpRu[P(OMe)$_3$](PPh$_3$)Cl (**5**).[38] The relative donor-ability of **1** [compared to PMe$_3$, P(OMe)$_3$, and P(OCH$_2$)$_3$CEt] was probed by comparing the Ru(III/II) redox potentials of TpRu(L)(PPh$_3$)Cl [L = P(OCH$_2$)$_2$(OCCH$_3$) (**2**), P(OCH$_2$)$_3$-CEt (**3**), PMe$_3$ (**4**), and P(OMe)$_3$ (**5**)] complexes (Chart 3).[31,38]

Chart 3. Ru(III/II) Potentials for TpRu(L)(PPh$_3$)Cl Complexes[a]

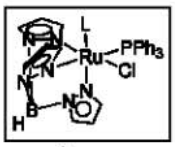

L				
Complex Number	(2)	(3)	(5)	(4)
$E_{1/2}$	1.08	0.95	0.88	0.75

[a]Data from cyclic voltammetry in NCCH$_3$ with reversible potentials ($E_{1/2}$) reported vs NHE (in V).

The Ru(III/II) potentials indicate the following trend in overall donor ability: PMe$_3$ > P(OMe)$_3$ > P(OCH$_2$)$_3$CEt > **1**. The Ru(III/II) potentials of complexes **2** and **3** differ by 0.13 V (1.08 and 0.95 V, respectively) with the potential of **2** positive compared to the potential of **3**, thus supporting the hypothesis that ligand **1** is less donating overall than P(OCH$_2$)$_3$CEt.

(η^6-C$_6$H$_6$)Ru(L)Cl$_2$ Complexes. To gain further insight into the donor ability of **1**, we prepared a series of (η^6-C$_6$H$_6$)-Ru(L)Cl$_2$ complexes [L = PPh$_3$ (**6**), P(OMe)$_3$ (**7**), PMe$_3$ (**8**), P(OCH$_2$)$_3$CEt (**9**), CO (**10**), and P(OCH$_2$)$_2$(OCCH$_3$) (**11**)] (Chart 2).[39 45] The syntheses of complexes **6**, **7**, and **10** have been previously reported.[39,40] A procedure similar to the synthesis of complex **7** was followed in the preparation of complexes **8**, **9**, and **11**, which involves stirring commercially available [(η^6-C$_6$H$_6$)Ru(Cl)(μ-Cl)]$_2$ with excess L in dichloro-methane (eq 3).

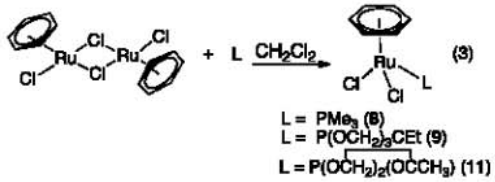

A single crystal of **11** suitable for an X-ray diffraction study was grown (Figure 2). The phosphite ligand of **11** has features that are similar to complex **2**. For example, there is one larger [102.5(1)] and two smaller [95.77(9) and 96.38(1)] O P O angles. The C3 O1 P1 angle [96.89(1)] is substantially smaller than the other two C O P angles, which are 106 .

dx.doi.org/10.1021/ic300109b | Inorg. Chem. 2012, 51, 4791 4801

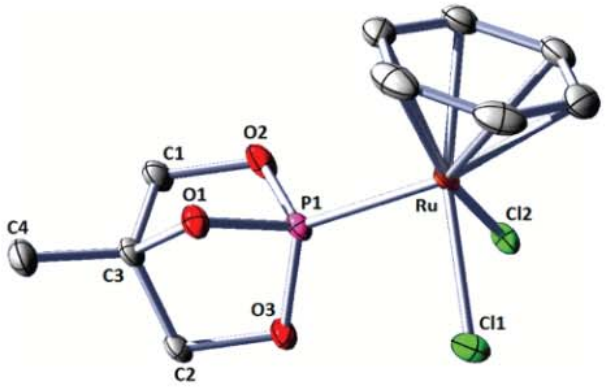

Figure 2. ORTEP diagram of $(\eta^6\text{-}C_6H_6)Ru[P(OCH_2)_2(OCCH_3)]Cl_2$ (**11**) (50% probability with hydrogen atoms omitted). Selected bond lengths (Å): Ru P1, 2.2453(7); P1 O1, 1.615(2); P1 O2, 1.616(2); P1 O3, 1.607(2); Avg. $C_{(C6H6)}$ Ru, 2.198(1). Selected bond angles (deg): O1 P1 O2, 95.77(9); O3 P1 O1, 96.38(1); O3 P1 O2 102.5(1); Cl1 Ru Cl2, 87.33(2); P1 Ru Cl1, 88.66(2); P1 Ru Cl2, 84.03(2); C3 O1 P1 96.89(1); C1 O2 P1 106.58(1); C2 O3 P1 106.24(1).

The cone angle of $P(OCH_2)_2(OCCH_3)$ calculated from the structure of complex **11** is 104 , which is identical to that determined using the structure of complex **2**. The average P O bond distances for **11** [1.613(2) Å] are longer than those for the $P(OCH_2)_3CEt$ complex **3** [1.605(2) Å], but not as long as those of complex **2** [1.627(3) Å, see above]. Table 3 shows some comparative geometric data for complexes **2**, **11**, and the previously reported complex $(\eta^6\text{-}C_6H_6)Ru[P(OMe)_3]Cl_2$ (**7**).[41]

Table 3. Selected Bond Lengths and Angles Comparing of 2, 7, and 11[a]

complex	O P O (deg)	C O P (deg)	O P Ru (deg)	P O (Å)
2	100.2(1)	97.5(2)	118.5(1)	1.627(3)
	94.6(1)	107.3(2)	126.2(1)	1.632(3)
	95.0(1)	107.4(2)	116.8(1)	1.620(3)
7	107.0(2)	123.1(3)	111.2(1)	1.565(3)
	98.7(2)	131.4(3)	123.4(1)	1.569(3)
	97.5(2)	119.4(3)	115.7(1)	1.594(3)
11	102.5(1)	96.89(1)	121.20(7)	1.615(2)
	95.77(9)	106.58(1)	120.98(6)	1.616(2)
	96.38(1)	106.24(1)	115.31(8)	1.607(2)

[a]The structure of **7** has been previously reported.[41]

The $(\eta^6\text{-}C_6H_6)Ru(L)Cl_2$ complexes were studied using cyclic voltammetry (Chart 4). For $(\eta^6\text{-}C_6H_6)Ru^{II}$ complexes, irreversible Ru(III/II) potentials are often observed, possibly because of dissociation of the benzene ligand in the oxidized Ru(III) state.[44] For the $(\eta^6\text{-}C_6H_6)Ru(L)Cl_2$ complexes studied herein, some complexes exhibit quasi-reversible Ru(III/II) potentials while others have chemically irreversible potentials. To standardize comparisons, we use $E_{p,a}$ and $E_{p,c}$ in the discussions below since the redox waves for complexes **9**, **10**, and **11** are not reversible. The carbonyl complex $(\eta^6\text{-}C_6H_6)Ru(CO)Cl_2$ (**10**), with $E_{p,a}$ = +1.78 V (vs NHE), was used as a benchmark to compare the donor ability of **1** because of the strong π-acidity of the CO ligand. The $E_{p,a}$ for complex **11** (1.50 V) is 0.28 V more negative than the $E_{p,a}$ for the CO complex **10**, indicating that the phosphite **1** is more donating than CO. Consistent with the $TpRu(L)(PPh_3)Cl$ complexes (see above), the Ru(III/II) potentials for the $(\eta^6\text{-}C_6H_6)Ru(L)Cl_2$ complexes indicate the following trend in overall donating ability: PMe_3 (complex **8**) > $P(OMe)_3$ (complex **7**) > $P(OCH_2)_3CEt$ (complex **6**) PPh_3 (complex **9**) > $P(OCH_2)_2(OCCH_3)$ (complex **11**) (Chart 4). Of the phosphines and phosphites studied, complex **11** yields a metal center with the most positive potential with $E_{p,a}$ = 1.50 V.

In addition to the Ru(III/II) potentials, a cathodic wave ($E_{p,c}$) is observed for each $(\eta^6\text{-}C_6H_6)Ru(L)Cl_2$ complex (Chart 4). The $P(OMe)_3$ complex **7** displays a two-electron reduction at 0.94 V.[46] Two one-electron reductions are observed for complex **6**, at $E_{p,a}$ = 0.85 and 1.07 V. All of the other complexes exhibit single-electron reductions. As the electron density of the metal center decreases, one would expect the $E_{p,c}$ to become less negative. Indeed, complexes **10** and **11** have the least negative reduction potentials, 0.50 and 0.99 V, respectively.

$(\eta^6$-p-cymene)Ru(L)Cl_2 Complexes. Another group of metal complexes containing phosphites/phosphines is $(\eta^6$-*p*-cymene)$Ru(L)Cl_2$.[5,47–49] Similar to the $(\eta^6\text{-}C_6H_6)Ru(L)Cl_2$, the complexes $(\eta^6$-*p*-cymene)$Ru[P(OCH_2)_3CEt]Cl_2$ (**12**), $(\eta^6$-*p*-cymene)$Ru[P(OCH_2)_2(OCCH_3)]Cl_2$ (**13**), $(\eta^6$-*p*-cymene)-$Ru[P(OMe)_3]Cl_2$ (**14**), and $(\eta^6$-*p*-cymene)$Ru(PPh_3)Cl_2$ (**15**) were synthesized by the reaction of $[(\eta^6$-*p*-cymene)$Ru(Cl)(\mu Cl)]_2$ with excess L in dichloromethane (eq 4).

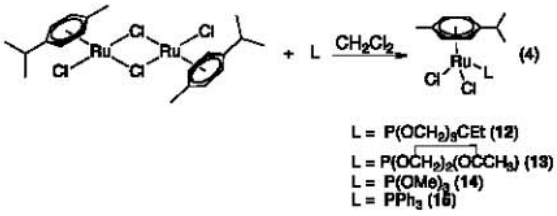

A single crystal suitable for X-ray diffraction was grown of complex **12** (Figure 3). On the basis of previously reported data, the Ru P bond distance increases with the following trend $P(OCH_2)_3CEt$ (**12**) < $P(OPh)_3$ < PPh_3 (**15**) < $P(NC_4H_4)_3$ (Table 4).[5,47,49] Furthermore, when comparing the O P O bond angles of complexes **2**, **11**, and **12**, removal of the methylene group to form phosphite **1** results in a substantial decrease in one of the O P O bond angles by approximately 5 . The Ru P bond length for complex **12** [2.2529(4) Å] is longer than that for complex **2** [2.191(1) Å] and **11** [2.2453(7) Å]. Additionally, the average P O bond lengths for complex **2** (1.626 Å) and **11** (1.613 Å) are longer than complex **12** (1.597 Å), consistent with phosphite **1** being a better π-acid than $P(OCH_2)_3CEt$.

Complexes **12** **15** were studied using cyclic voltammetry (Chart 5). It was determined that the least electron density on the metal center is observed for complex **13** where $E_{1/2}$ = 1.44, $E_{p,a}$ = 1.47 V and $E_{p,c}$ = 1.44 V. This observation is consistent with data collected for the $\eta^6\text{-}C_6H_6$ systems (see above). When using $E_{1/2}$ values the same trend is apparent (Chart 5).

Kinetic Studies for Phosphine/Phosphite Exchange. As a final probe of the properties of **1** as a ligand, we compared the rate of exchange of L with $P(OMe)_3$ for $(\eta^6$-*p*-cymene)-$Ru(L)Cl_2$ complexes [L = **1**, $P(OCH_2)_3CEt$ and PPh_3]. The exchange rates were determined under pseudofirst-order conditions by monitoring the disappearance of $(\eta^6$-*p*-cymene)-$Ru(L)Cl_2$ in the presence of excess $P(OMe)_3$ with ^1H NMR spectroscopy. Figure 4 displays plots of concentration of Ru

dx.doi.org/10.1021/ic300109b | Inorg. Chem. 2012, 51, 4791 4801

Chart 4. Ru(III/II) Potentials for $(\eta^6\text{-}C_6H_6)Ru(L)Cl_2$ Complexes[a]

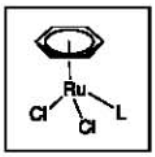

L	CO				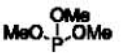	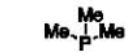
Complex Number	(10)	(11)	(6)	(9)	(7)	(8)
$E_{1/2}$	-	-	1.31	-	1.30	1.19
$E_{p,a}$	1.78	1.50	1.40[b]	1.39	1.34[b]	1.24[b]
$E_{p,c}$	-0.50	-0.99	-1.07 -0.85	-1.09	-0.94 (n = 2)	-1.25

[a]Data from cyclic voltammetry in $NCCH_3$ with potentials reported vs NHE (in V). [b]Denotes quasi-reversible potential.

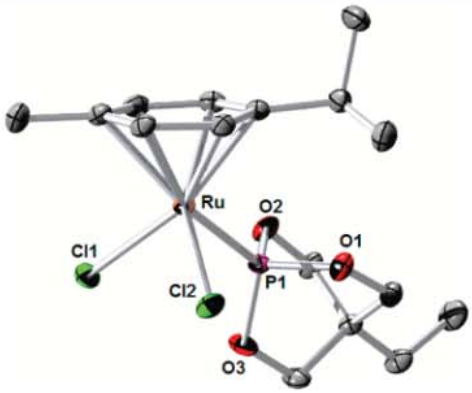

Figure 3. ORTEP of $(\eta^6\text{-}p\text{-cymene})Ru[P(OCH_2)_3CEt]Cl_2$ (**12**) (50% probability with hydrogen atoms omitted). Selected bond lengths (Å): Ru P1, 2.2529(4); P1 O1, 1.599(1); P1 O2, 1.599(1); P1 O3, 1.594(1). Selected bond angles (deg): O3 P1 O2, 102.82(6); O3 P1 O1, 102.37(6); O2 P1 O1, 102.31(6); Cl1 Ru Cl2, 88.59(1); P1 Ru Cl1, 88.10(1); P1 Ru Cl2, 83.91(1).

Table 4. Comparison of Bond Lengths from Crystallographic Data for $(\eta^6\text{-}p\text{-cymene})Ru(L)Cl_2$ Complexes

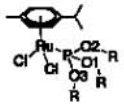

P-Ligand	Ru P1 (Å)	P1 O1 (Å)	P1 O2 (Å)	P1 O3 (Å)
PPh_3	2.3438(6)	*a*	*a*	*a*
$P(OCH_2)_3CEt$	2.2529(4)	1.599(1)	1.599(1)	1.594(1)
$P(NC_4H_4)_3$	2.396(2)	*a*	*a*	*a*
$P(OPh)_3$	2.2642(8)	1.596(2)	1.607(2)	1.584(2)

[a]No oxygen atom in P-based ligand.

complex vs time for **12**, **13**, and **15**. The k_{obs} values for each reaction were determined by fitting the plots to first-order decays, which gives the following relative k_{obs} magnitudes: **15** [k_{obs} = 0.0045(3) s ^{1}] > **13** [k_{obs} = 0.0030(1) s ^{1}] **12** [k_{obs} = 8.5(6) 10 ^{5} s ^{1}].

Figure 5 shows a plot of k_{obs} vs concentration of PPh_3 for the reaction of **15** with $P(OMe)_3$. Increasing the concentration of PPh_3 decreases the rate of ligand exchange indicating an inverse rate dependence on concentration of PPh_3. Figure 6 displays a plot of k_{obs} vs concentration of $P(OMe)_3$ for the reaction of **15**

Chart 5. Ru(III/II) Potentials for $(\eta^6\text{-}p\text{-cymene})Ru(L)Cl_2$ Complexes[a]

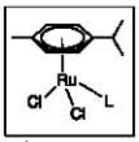

L			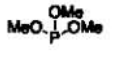	
Complex Number	(13)	(12)	(14)	(15)
$E_{1/2}$	1.44	1.30	1.25	1.25
$E_{p,a}$	1.47[b]	1.35[b]	1.30[b]	1.29
$E_{p,c}$	-1.05	-1.23	-1.21	-1.25

[a]Data from cyclic voltammetry in $NCCH_3$ with potentials reported vs NHE (in V). [b] Denotes quasi-reversible potential.

with $P(OMe)_3$. The rate of reaction initially increases, and saturation is observed at higher concentrations of $P(OMe)_3$. Scheme 2 shows a potential reaction pathway for the conversion of **12**, **13**, or **15** and $P(OMe)_3$ to $(\eta^6\text{-}p\text{-cymene})Ru[P(OMe)_3]Cl_2$ that is consistent with the kinetic data for the reaction of **15** and $P(OMe)_3$ (see the rate law shown in eq 5 for

$$\text{Rate} = \frac{k_1 k_2[P(OMe)_3][\text{Ru Complex}]}{k_{-1}[L] + k_2[P(OMe)_3]} \quad (5)$$

this pathway). Since **12**, **13**, and **15** are 18-electron complexes, a ligand exchange by a dissociative pathway is reasonable. Under saturation conditions {where $k_2[P(OMe)_3] > k_{-1}[L]$}, the rate law can be reduced to rate = k_1[Ru complex] where $k_{obs} = k_1$, which is the rate constant for dissociation of L. Thus, the k_{obs} values derived from the kinetic plots in Figure 4 should provide relative rates of dissociation of L from $(\eta^6\text{-}p\text{-cymene})Ru(L)Cl_2$ complexes. The k_{obs} values indicate that the rate of dissociation of **1** is similar to that of PPh_3, and that **1** and PPh_3 dissociate more rapidly than $P(OCH_2)_3CEt$.

Calculations: Bicyclic Phosphite π-Acidity. To further understand the bonding between **1** and transition metals, density functional theory (DFT) calculations were carried out to compare bonding of **1** to $P(OMe)_3$, $P(OCH_2)_3CEt$, and PF_3. The role of the P X (X = O, C, halide, etc.) σ^* orbitals in

dx.doi.org/10.1021/ic300109b | Inorg. Chem. 2012, 51, 4791 4801

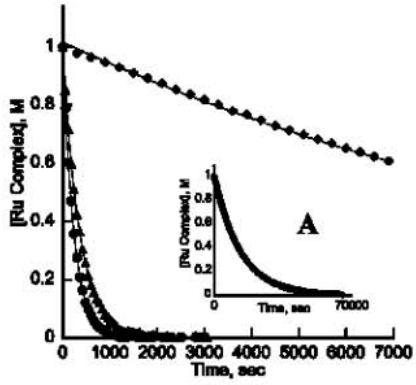

Figure 4. Representative kinetic plots for the exchange reaction of L in (η^6-*p*-cymene)Ru(L)Cl_2 complexes with $P(OMe)_3$ (40 equiv relevant to concentration of Ru complex) in $CDCl_3$ at 60 C [L = $P(OCH_2)_2(OCCH_3)$ (**13**) [k_{obs} = 0.0030(1) s ^{1}, R^2 = 0.99], PPh_3 (**15**) [k_{obs} = 0.0045(3) s ^{1}, R^2 = 0.99)], $P(OCH_2)_3CEt$ (**12**) [k_{obs} = 0.000085(6) s ^{1}, R^2 = 0.99]. Plot **A** shows the entire plot for the exchange reaction with L = $P(OCH_2)_3CEt$ (**12**).

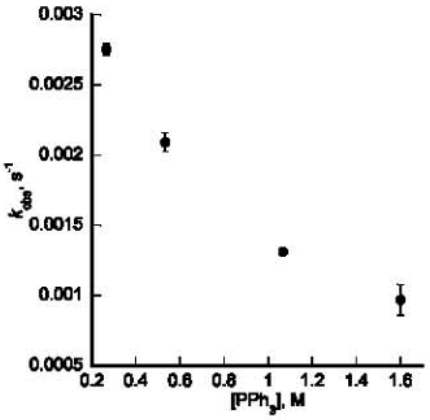

Figure 5. Plot of k_{obs} versus concentration of PPh_3 for the exchange of PPh_3 with $P(OMe)_3$ upon reaction of (η^6-*p*-cymene)Ru(PPh_3)Cl_2 (**15**) with excess $P(OMe)_3$ in $CDCl_3$ at 60 C.

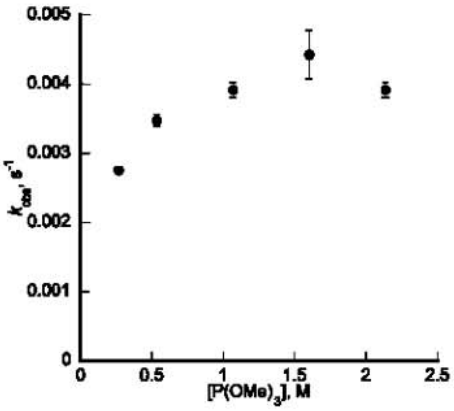

Figure 6. Plot of k_{obs} versus concentration of $P(OMe)_3$ for the exchange of PPh_3 with $P(OMe)_3$ upon reaction of (η^6-*p*-cymene)Ru-(PPh_3)Cl_2 (**15**) with excess $P(OMe)_3$ in $CDCl_3$ at 60 C.

Scheme 2. Proposed Mechanism for Exchange Reaction of L with $P(OMe)_3$ to Form (η^6-*p*-cymene)Ru[$P(OMe)_3$]Cl_2 in $CDCl_3$ at 60 C

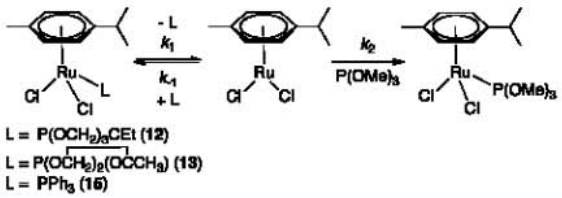

π-acidity of phosphorus ligands has been documented.[9,50,51] The energies of the PX_3 σ^* orbitals are a function of the substituent X as well as the X P X bond angle.[1,9] Smaller X P X angles are suggested to result in better π-acceptor ligands as the lowest unoccupied molecular orbitals (LUMOs) are lower in energy because of the reduced overlap between the 3p phosphorus orbitals with σ-orbitals of the X substituents. Thus, the decreased O P O bond angles of bicyclic phosphites that result from the cyclic structure are expected to decrease the energy of the σ^* orbitals and, as a result, enhance π acidity.

Structures were optimized for a linear gold(I) complex [AuCl(L)] and for the free ligand L where L = **1**, $P(OMe)_3$, $P(OCH_2)_3CEt$, or PF_3. AuCl(L) is an established organometallic fragment used by Fey et al. to parametrize ligand electronic and steric effects.[52] While the experimental studies herein are focused on Ru(II), the d^{10} configuration of the Au(I) complex allowed for easier delineation of σ-donor and π-acceptor electronic effects without steric influence from *cis* ligands. The free ligand highest occupied molecular orbital (HOMO) and LUMO energies (E_{HOMO} and E_{LUMO}) are given in Table 5, along with the Au P bond length and phosphine substituent angles (X P X) from the [AuCl(L)] complexes.

Care was taken when modeling the conformation of $P(OMe)_3$,[53] with the lowest energy conformers in low and high coordinate compounds investigated (ag^+g^+ and ag^+g^+ respectively), as well as the most similar $P(OMe)_3$ conformation to **1**, where the OMe groups are all *anti* to the metal phosphorus bond (*aaa*) (Scheme 3). Consideration of conformations is important to ensure that possible anomeric effects are not neglected,[54] as delocalization of the phosphorus lone pair into an O C σ^* orbital is known to be more favorable if the substituent has an *anti* configuration.[55] The anomeric effect is lessened when the phosphite is coordinated to a metal center.[53]

The descriptor E_{LUMO} has been shown in Ligand Knowledge Base research to be related to the π-accepting character of a phosphorus ligand.[52] As the results in Table 5 indicate, the energy of the LUMO (E_{LUMO}) is significantly lower for **1** compared to that of the $P(OMe)_3$ conformers, which directly correlates to the size of the O P O angle. Likewise, the E_{LUMO} of **1** is lower than that calculated for $P(OCH_2)_3CEt$. The calculated X P X angles of **1** and PF_3 are smallest, supporting the hypothesis that small X P X angles lower the E_{LUMO} and thereby increase the ligand s π -acidity. The LUMO energy for PF_3 is likely lower than that for **1** as a result of the more strongly withdrawing fluorine substituents of PF_3. Structural parameters from the linear Au(I) calculations also show a clear correlation between the E_{LUMO}, Au P bond lengths, and the NBO analysis for the 3s character of P, all given in Table 5. For the latter, **1** has more s character for the phosphorus lone pair than the other phosphite ligands studied, with PF_3, as expected, exhibiting the largest s character as it is the best π-acceptor. Again for **1**, Au P is shorter (0.02 Å) than that observed in

dx.doi.org/10.1021/ic300109b | Inorg. Chem. 2012, 51, 4791 4801

Table 5. Data from DFT Calculations of $P(\overline{OCH_2)_2(OCCH_3})$ (1), $P(OMe)_3$, $P(OCH_2)_3CEt$, and PF_3

ligand	conformation	E_{HOMO} [hartree]	E_{LUMO} [hartree]	Au P [Å]	NBO 3s character on P	average X P X [deg]	relative free energy [kcal mol ^{1}]
$P(\overline{OCH_2)_2(OCCH_3})$ (1)		0.2343	0.0428	2.21	1.564	97.4	
$P(OMe)_3$	ag^+g^+	0.2190	0.0235	2.24	1.541	102.5	0.0
$P(OMe)_3$	ag^-g^+	0.2230	0.0241	2.24	1.544	102.7	1.0
$P(OMe)_3$	*aaa*	0.2215	0.0118	2.23	1.538	105.6	7.6
$P(OCH_2)_3CEt$		0.2296	0.0196	2.22	1.531	102.2	
PF_3		0.3089	0.0709	2.20	1.652	99.5	

Scheme 3. Orientations of $P(OMe)_3$ Ligand Defined by the Torsion Au P O Me (Viewed along the Au P Bond) That Were Modeled Using DFT Calculations

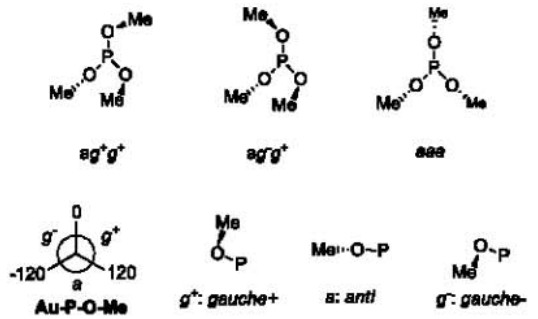

the equivalent $P(OMe)_3$ and $P(OCH_2)_3CEt$ complexes, further corroborating a higher π-acidity character for phosphite **1** than the others included in this study and placing it below PF_3 on the π-acidity scale.

CONCLUSIONS

Crystallographic and cyclic voltammetry data have been used to demarcate the properties of **1** compared with other phosphine and phosphite ligands, as well as carbon monoxide, using three types of ruthenium complexes, $TpRu(L)(PPh_3)Cl$, $(\eta^6\text{-}C_6H_6)$-$Ru(L)Cl_2$, and $(\eta^6\text{-}p\text{-cymene})Ru(L)Cl_2$. Data clearly indicate that the formal removal of one methylene group from the bicyclic phosphite $P(OCH_2)_3CEt$, which gives phosphite **1**, results in a decrease in electron-density at the metal center. For all three types of Ru complexes, redox potentials with **1** in the coordination sphere are shifted positive by 0.11 to 0.13 V compared to analogous systems with $P(OCH_2)_3CEt$. Furthermore, when L = **1**, the metal is less electron-rich (as determined by cyclic voltammetry) than metals coordinated by all other phosphorus ligands studied including $P(OMe)_3$, PMe_3, PPh_3, and $P(OCH_2)_3CEt$. It can be concluded that **1** is overall more weakly donating than the acyclic phosphite $P(OMe)_3$. The source of these differences is more difficult to pinpoint. Verkade et al. have rationalized differences in basicity of cyclic vs acyclic phosphites (and related ligands) with the hinge effect,[3,23 26] which involves differences in O P π-overlap as function of O P O and P O C bond angles (see above). In addition, differences in O P O bond angles (for cyclic vs acyclic phosphites) might impact O P σ-overlap and, hence, the energy of P O σ^* orbitals, which could influence ligand π-acidity. DFT calculations are consistent with this suggestion and indicate a lower energy LUMO for **1** compared to $P(OMe)_3$ and $P(OCH_2)_3CEt$.

EXPERIMENTAL SECTION

General Methods. Unless otherwise noted, all synthetic procedures were performed under anaerobic conditions in a nitrogen-filled glovebox or by using standard Schlenk techniques. Glovebox purity was maintained by periodic nitrogen purges and was monitored by an oxygen analyzer [O_2(g) < 15 ppm for all reactions]. Tetrahydrofuran was dried by distillation from sodium/benzophenone. Pentane was distilled over P_2O_5. Acetonitrile and diethyl ether were dried by distillation from CaH_2. Hexanes, benzene, and methylene chloride were purified by passage through a column of activated alumina. Benzene-d_6, acetonitrile-d_3, methylene chloride-d_2, and chloroform-d_1 were stored under a N_2 atmosphere over 4 Å molecular sieves. ^{1}H NMR spectra were recorded on a Varian Mercury 300 or 500 MHz spectrometer, and ^{13}C NMR spectra were recorded on a Varian Mercury 500 MHz spectrometer (operating frequency 125 MHz). All ^{1}H and ^{13}C NMR spectra are referenced against residual proton signals (^{1}H NMR) or the ^{13}C resonances of the deuterated solvent (^{13}C NMR). ^{31}P NMR spectra were obtained on a Varian 300 MHz (operating frequency 121 MHz) spectrometer and referenced against an external standard of H_3PO_4 (δ = 0). Resonances due to the Tp ligand in ^{1}H NMR spectra are listed by chemical shift and multiplicity only (all coupling constants for the Tp ligand are 2 Hz).

Electrochemical experiments were performed under a nitrogen atmosphere using a BAS Epsilon Potentiostat. Cyclic voltammograms were recorded in $NCCH_3$ using a standard three electrode cell from 1700 to 1700 mV at 100 mV/s [with the exception of $(\eta^6\text{-}C_6H_6)Ru(CO)Cl_2$, which was scanned from 1700 to 2500 mV at a scan rate of 100 mV/s] with a glassy carbon working electrode and tetrabutylammonium hexafluorophosphate as electrolyte. All potentials are reported versus NHE (normal hydrogen electrode) using ferrocene as the internal standard.

High-resolution electrospray ionization mass spectrometry (ESI-MS) analyses were obtained on a Bruker BioTOF-Q spectrometer at the University of Richmond. Samples were dissolved in acetonitrile then mixed 3:1 with 0.1 M aqueous sodium trifluoroacetate (NaTFA) using $[Na(NaTFA)_x]^+$ clusters as an internal standard. These data are reported using the most intense peaks from the isotopic envelope for $[M + Na]^+$. The data are listed as m/z with the intensity relative to the most abundant peak of the isotopic envelope given in parentheses for both the calculated and the observed peaks. The difference between calculated and observed peaks is reported in ppm. In all cases, observed isotopic envelopes were consistent with the composition reported.

The preparation, isolation, and characterization of $TpRu[P(OCH_2)_3CEt](PPh_3)Cl$ (**3**),[31] $TpRu(PMe_3)(PPh_3)Cl$ (**4**),[38] $(\eta^6\text{-}C_6H_6)Ru(CO)Cl_2$ (**11**),[39] $(\eta^6\text{-}C_6H_6)Ru(PPh_3)Cl_2$ (**6**),[40] and $(\eta^6\text{-}C_6H_6)Ru[P(OMe)_3]Cl$ (**7**)[40] have been previously reported. $P(OCH_2)_3CEt$ was obtained from a commercial source and purified by reconstitution in hexanes followed by filtration through Celite. The filtrate was concentrated to dryness to yield pure material.

Calculations. DFT calculations were performed using the standard Becke-Perdew (BP86) density functional[56 60] in conjunction with the double-ζ 6-31+G(d) basis set for all atoms excluding gold, for which the Los Alamos National Laboratory LANL2DZ[61] basis set, augmented by diffuse and contracted f functions taken from Pyykko and Mendizabal[62] and the 6p functions of Couty and Hall,[63] was

dx.doi.org/10.1021/ic300109b | Inorg. Chem. 2012, 51, 4791 4801

employed. All calculations were performed using the Gaussian 09 suite of programs.[64]

$C(CH_3)(OH)(CH_2OH)_2$. The synthesis of $C(CH_3)(OH)(CH_2OH)_2$ has been previously reported.[36] We used an alternate procedure. The reaction was performed in a vented hood. H_2O_2 (30%, 6.82 mL, 0.0662 mol) was added to formic acid (88%, 27.8 mL, 0.648 mol), and the mixture was stirred at room temperature for 5 min. The flask was placed in an ice bath, and 2-methyl-2-propen-1-ol (4.0 mL, 0.047 mol) was added slowly using an addition funnel. The reaction was heated at 40 C for 1 h. The solution was allowed to cool to room temperature. After 16 h at room temperature, the solution was concentrated in vacuo, and the residual oil was cooled in an ice bath and treated dropwise with 10 mL of cold NaOH (13.3 M). The resulting mixture was heated for 1 h at 40 C, which resulted in a yellow solution. After the addition of acetone (50 mL), the top layer was removed using a pipet. The acetone addition/extraction was repeated three times, and all extractions were combined. The combined fractions were concentrated under reduced pressure. The remaining pale yellow viscous oil was dissolved in a minimal amount of methanol, and diethyl ether was added to induce precipitation. The mixture was filtered using a fine porosity frit, and the solid was discarded. This step was repeated multiple times until no precipitate was observed upon the addition of diethyl ether. The filtrates were combined and concentrated in vacuo to give a brownish-yellow oil. The oil was purified by column chromatography on silica using 1:2 methanol/ethyl acetate as eluent. The solution was concentrated to dryness to yield a brownish-yellow oil (2.634 g, 84%). The sample was dried by azeotropic distillation in benzene. ^{1}H NMR (D_2O, 300 MHz, δ) 3.47 (s, 4H, CH_2), 1.13 (s, 3H, CH_3). ^{13}C NMR (125 MHz, CD_3OD, δ) 73.8, 67.6 (both s, *C* and CH_2), 21.3 (s, CH_3).

$P(O\overline{CH_2)_2(OCCH_3}$)(1). The synthesis of $P(O\overline{CH_2)_2(OCCH_3})$ has been previously reported.[33] We used a modified procedure. $C(CH_3)(OH)(CH_2OH)_2$ (1.032 g, 9.725 mmol) was added to benzene (200 mL) in a 400 mL beaker. NaH (0.695 g, 29.0 mmol) was added to the reaction vessel, and the reaction mixture was stirred at room temperature for 1.25 h. PCl_3 (775 μL, 8.89 mmol) was added slowly via syringe, and the reaction was stirred at room temperature overnight. The heterogeneous mixture was filtered through a fine porosity frit. Attempts to isolate pure **1** resulted in decomposition. Thus, for coordination to Ru, **1** was generated as described above and added to the Ru precursor without isolation. ^{31}P{^{1}H} NMR (121 MHz, C_6D_6, δ): 115.5.

TpRu[$P(O\overline{CH_2)_2(OCCH_3}$)](PPh$_3$)Cl (2). A benzene solution of **1** (150 mL, 2.98 mmol) was added to $TpRu(PPh_3)_2Cl$ (0.510 g, 0.564 mmol). The solution was refluxed for 3 h to give a bright yellow solution. The solution was filtered through Celite, and the volatiles were removed from the filtrate in vacuo. The resulting solid was dissolved in minimal THF. Hexanes were added to induce precipitation of a yellow solid, which was collected on a fine porosity frit and dried in vacuo. The solid was dissolved in CH_2Cl_2 and loaded onto a silica column. The column was washed with hexanes, and the eluent was discarded. The column was then washed with Et_2O. The eluent was collected and reduced in vacuo to 2 mL. Hexanes were added to induce precipitation of a yellow solid, which was collected on a fine porosity frit and dried in vacuo (0.0933 g, 19.5% yield). Crystals of **2** were obtained by slow evaporation of a CH_2Cl_2 solution layered with hexanes. ^{1}H NMR (500 MHz, $CDCl_3$, δ): 8.15, 7.65, 7.63, 7.52 (each a d, each 1H, Tp 3 and 5), 7.38 7.15 (overlapping m s, 15H, $P(C_6H_5)_3$), 6.91, 6.72 (each a d, each 1H, Tp 3 and 5), 6.09 (dt, 1H, $^5J_{HP}$ = 1.0 Hz, Tp 4), 5.80 (dt, 1H, $^5J_{HP}$ = 1.3 Hz, Tp 4), 5.75 (t, 1H, Tp 4), 3.93 (dd, 2H, $^2J_{HH}$ = 8.0 Hz, $^3J_{HP}$ = 8.0 Hz, $P(O\overline{CH_2)_2(OCCH_3}$); Note: assignment of coupling constants was based on decoupling experiments), 3.50 (ddd, 1H, $^2J_{HH}$ = 8.0 Hz, $^3J_{HP}$ = 3.6 Hz, $^4J_{HH}$ = 1.4 Hz, $P(O\overline{CH_2)_2(OCCH_3}$)), 3.45 (ddd, 1H, $^2J_{HH}$ = 8.0 Hz, $^3J_{HP}$ = 3.6 Hz, $^4J_{HH}$ = 1.4 Hz, $P(O\overline{CH_2)_2(OCCH_3}$)), 1.51 (s, 3H, $P(O\overline{CH_2)_2(OCCH_3}$)). ^{13}C NMR (125 MHz, $CDCl_3$, δ): 148.2, 145.3, 143.9, 136.4 (Tp 3 or 5 position), 135.0 (d, J_{CP} = 9.0 Hz, *ortho* or *meta* of PPh_3), 134.7, 134.5 (Tp 3 or 5 or ipso of PPh_3 with one singlet missing presumably because of coincidental overlap), 129.3 (*para* of PPh_3), 127.4 (d, J_{CP} = 9.0 Hz, *ortho* or *meta* of PPh_3), 105.7, 105.5, 105.2 (Tp 4 position), 81.6 [$P(O\overline{CH_2)_2(OCCH_3}$)], 74.9 74.7 (overlapping resonances, $P(O\overline{CH_2)_2(OCCH_3}$)), 15.6 (d, J_{CP} = 10 Hz, $P(O\overline{CH_2)_2(OCCH_3}$)). ^{31}P{^{1}H} NMR (121 MHz, $CDCl_3$, δ): 162.6 (d, $^2J_{PP}$ = 55 Hz, $P(O\overline{CH_2)_2(OCCH_3}$)), 44.8 (d, $^2J_{PP}$ = 55 Hz, *P*Ph$_3$). CV ($NCCH_3$): $E_{1/2}$ = 1.08 V Ru(III/II). Anal. Calcd. for $C_{22}H_{35}BClN_6O_3P_2Ru$ CH_2Cl_2 [Note: repeated efforts to dry this sample did not remove residual solvent. Thus, one equivalent of dichloromethane (observed and quantified by ^{1}H NMR spectroscopy) is included in elemental analysis calculations]: C, 46.26; H, 4.12; N, 10.12. Found: C, 46.84; H, 4.19; N, 10.28.

TpRu[P(OMe)$_3$](PPh$_3$)Cl (5). $TpRu(PPh_3)_2Cl$ (0.295 g, 0.338 mmol) was added to 20 mL of C_6H_6, and $P(OMe)_3$ (0.0460 g, 0.371 mmol) was added. The solution was refluxed for 3 h to give a bright yellow solution. The volatiles were removed in vacuo. The resulting solid was dissolved in minimal THF. Hexanes were added, and the solvent was reduced in vacuo to induce precipitation of a yellow solid, which was collected on a fine porosity frit and dried in vacuo (0.0557 g, 67.0%). ^{1}H NMR (300 MHz, $CDCl_3$, δ) 8.12, 7.65, 7.58, 7.56 (each a d, each 1H, Tp 3 and 5), 7.41 7.11 (overlapping m s, 15H, $P(C_6H_5)_3$), 6.83, 6.66 (each a d, each 1H, Tp 3 and 5), 6.13, 5.75, 5.70 (each a t, each 1H, Tp 4), 3.24 (d, $^3J_{HP}$ = 10.3 Hz, 9H, $P(OCH_3)_3$). ^{13}C NMR (125 MHz, $CDCl_3$) δ 148.0, 144.8, 144.1, 136.2, 135.5, 135.2 (Tp 3 or 5 position), 134.9 (d, J_{CP} = 9 Hz, *ortho* or *meta* of $P(C_6H_5)_3$), 134.6 (ipso of $P(C_6H_5)_3$), 128.9 (*para* of $P(C_6H_5)_3$), 127.2 (d, J_{CP} = 9 Hz, *ortho* or *meta* of $P(C_6H_5)_3$), 105.2 (coincidental overlap of two Tp 4 position), 104.3 (Tp 4 position), 51.8 (d, $^2J_{CP}$ = 6.3 Hz, CH_3). ^{31}P NMR (121 MHz, $CDCl_3$, δ): 145.9 (d, $^2J_{PP}$ = 54 Hz, *P*(OMe)$_3$, 46.1 (d, $^2J_{PP}$ = 54 Hz, *P*Ph$_3$). CV ($NCCH_3$): $E_{1/2}$ = 0.88 V Ru(III/II). HRMS: $[M + Na]^+$ obsd (%), calcd (%), ppm: 756.091 (38), 756.08845 (31.1), 3.4; 757.09061 (50.3), 757.09029 (53), 0.4; 758.09062 (77), 758.08983 (78.8), 1; 759.08946 (100), 759.08712 (100), 3.1; 760.09086 (56.8), 760.08976 (49.2), 1.4; 761.08919 (73.4), 761.08741 (72.6), 2.3; 762.09149 (26.1), 762.0891 (27.9), 3.1.

(η^6-C_6H_6)Ru(PPh$_3$)Cl$_2$ (6). The synthesis and characterization of (η^6-C_6H_6)Ru(PPh_3)Cl_2 have been previously reported.[40] ^{1}H NMR spectroscopy revealed pure material and was consistent with previously reported data. CV ($NCCH_3$): $E_{1/2}$ = 1.31 V Ru(III/II) (quasi-reversible); $E_{p,c}$ = 0.85 V and 1.07 V)

(η^6-C_6H_6)Ru[P(OMe)$_3$]Cl (7). The synthesis and characterization of (η^6-C_6H_6)Ru[$P(OMe)_3$]Cl_2 have been previously reported.[40] ^{1}H NMR spectroscopy revealed clean material and was consistent with previously reported data. CV ($NCCH_3$): $E_{1/2}$ = 1.30 V Ru(III/II) (quasi-reversible); $E_{p,c}$ = 0.94 V (n = 2).

(η^6-C_6H_6)Ru(PMe$_3$)Cl$_2$ (8). The synthesis of (η^6-C_6H_6)Ru(PMe_3)-Cl_2 has been previously reported.[42] We used an alternate procedure. [(η^6-C_6H_6)Ru(Cl)(μ-Cl)]$_2$ (0.140 g, 0.280 mmol) was stirred in CH_2Cl_2 (30 mL) at room temperature. PMe_3 (0.0470 g, 0.616 mmol) was added slowly by syringe. The mixture was stirred at room temperature for 3 h during which time the heterogeneous mixture became a homogeneous red solution. The solution was filtered through a fine porosity frit. The filtrate was reduced in vacuo to 5 mL. Hexanes were added to provide an orange precipitate. The mixture was filtered through a fine porosity fritted funnel. The solid was dried in vacuo to yield an orange solid (0.153 g, 83.8%). Although complex **8** has been previously reported, NMR data were not provided. ^{1}H NMR (500 MHz, $CDCl_3$, δ): 5.58 (s, 6H, C_6H_6), 1.65 (d, 9H, $^2J_{HP}$ = 11.4 Hz, CH_3). ^{13}C NMR (125 MHz, $CDCl_3$, δ): 87.2 (s, C_6H_6), 16.6 (d, $^1J_{PC}$ = 34.1 Hz, CH_3) ^{31}P{^{1}H} NMR (121 MHz, $CDCl_3$, δ): 7.5 (s, *P*Me$_3$). CV ($NCCH_3$): $E_{1/2}$ = 1.19 V Ru(III/II) (quasi-reversible); $E_{p,c}$ = 1.25 V.

(η^6-C_6H_6)Ru[P(OCH$_2$)$_3$CEt]Cl$_2$ (9). $P(OCH_2)_3CEt$ (0.248 g, 1.53 mmol) and [(η^6-C_6H_6)Ru(Cl)(μ-Cl)]$_2$ (0.382 g, 0.764 mmol) were stirred in CH_2Cl_2 (50 mL) at room temperature overnight to give a heterogeneous mixture. The solid was collected by filtration

dx.doi.org/10.1021/ic300109b | Inorg. Chem. 2012, 51, 4791 4801

through a fine porosity frit, washed with CH_2Cl_2 and pentane, and dried in vacuo to yield a red solid (0.601 g, 95.5%). ^{1}H NMR (500 MHz, DMSO-d_6, δ): 5.82 (s, 6H, C_6H_6), 4.37 (d, 6H, $^3J_{HP}$ = 4.7 Hz, $P(OCH_2)_3CCH_2CH_3$), 1.24 (q, 2H, $^3J_{HH}$ = 7.7 Hz, CCH_2CH_3), 0.77 (t, 3H, $^3J_{HH}$ = 7.6 Hz, CCH_2CH_3). ^{13}C NMR (125 MHz, DMSO-d_6, δ): 90.0 (s, C_6H_6), 87.6 (s, $P(OCH_2)_3CCH_2CH_3$), 74.8 (s, $P(OCH_2)_3CCH_2CH_3$), 22.1 (s, $P(OCH_2)_3CCH_2CH_3$), 6.9 (s, $P(OCH_2)_3CCH_2CH_3$). ^{31}P{^{1}H} NMR (121 MHz, DMSO-d_6, δ): 107.5 (s, $P(OCH_2)_3CCH_2CH_3$). CV ($NCCH_3$): $E_{p,a}$ = 1.39 V Ru(III/II); $E_{p,c}$ = 1.09 V Ru(II/I). Anal. Calcd for $C_{12}H_{17}Cl_2O_3PRu(CH_2Cl_2)_{0.25}$ [Note: repeated efforts to dry this sample did not remove residual solvent. Thus, 0.25 equivalents of dichloromethane (observed and quantified by ^{1}H NMR spectroscopy) are included in elemental analysis calculations]: C, 33.94; H, 4.08. Found: C, 34.25; H, 4.18.

(η^6-C_6H_6)Ru[P(OCH$_2$)$_2$(OCCH$_3$)]Cl$_2$ (11). Compound **1** [55 mL of **1** in C_6H_6 (0.0054 M)] was added to $[(\eta^6\text{-}C_6H_6)Ru(Cl)(\mu\text{-}Cl)]_2$ (0.505 g, 1.01 mmol). The solution was stirred in CH_2Cl_2 (100 mL) at room temperature for 2 h to give an orange solution. The mixture was filtered through a fine porosity frit. The filtrate was added to a 1/4 in. plug of silica gel on top of 1/4 in. of Celite and eluted with CH_2Cl_2. The volume of the eluent was reduced in vacuo to 3 mL. Hexanes were added to the eluent to yield a red precipitate. The solution was filtered through a fine porosity frit and dried in vacuo to give a red solid (0.102 g, 25% based on Ru dimer). Crystals of **4** were obtained by slow evaporation from a chloroform solution. ^{1}H NMR (500 MHz, CD_2Cl_2, δ) 5.90 (s, 6H, C_6H_6), 4.26 (m, 2H, $P(OCH_2)_2(OCCH_3)$), 3.84 (d, 2H, $^2J_{HH}$ = 6.5 Hz CH_2), 1.69 (s, 3H, CH_3). ^{13}C NMR (75 MHz, $CDCl_3$, δ): 91.5 (s, C_6H_6), 83.3 (s, $P(OCH_2)_2(OCCH_3)$), 75.9 (d, $^2J_{CP}$ = 5.4 Hz, $P(OCH_2)_2(OCCH_3)$), 15.0 (s, $P(OCH_2)_2(OCCH_3)$). ^{31}P{^{1}H} NMR (121 MHz, CD_2Cl_2, δ): 139.7 $P(OCH_2)_2(OCCH_3)$. HRMS: $[M + Na]^+$ obsd (%), calcd (%), ppm: 403.89292 (36.8), 403.8932 (15.2), 0.7; 405.89292 (36.8), 405.89274 (25.3), 0.4; 406.89271 (100), 406.8917 (100), 2.5; 407.89157 (36.8), 407.89134 (12.8), 0.6; 408.88907 (97.7), 408.89079 (28.8), 4.2; 409.89174 (85.5), 409.8919 (84.2), 0.4; 410.88847 (85.5), 410.88871 (84.2), 0.6. CV ($NCCH_3$): $E_{p,a}$ = 1.50 V Ru(III/II); $E_{p,c}$ = 0.99 V Ru(II/I).

(η^6-p-cymene)Ru[P(OCH$_2$)$_3$CEt]Cl$_2$ (12). The dimeric complex $[(\eta^6\text{-}p\text{-cymene})Ru(Cl)(\mu\text{-}Cl)]_2$ (0.102 g, 0.166 mmol) and $P(OCH_2)_3CEt$ (0.0690 g, 0.436 mmol) were combined in a round-bottom flask with 20 mL of CH_2Cl_2. The reaction mixture was stirred at room temperature for 1 h. The total volume of the solution was reduced in vacuo to 2 mL. Hexanes were added to yield a red-orange precipitate. The solid was collected by filtration through a fine porosity frit and dried in vacuo to yield a red-orange solid (0.3830 g, 83%). ^{1}H NMR (300 MHz, $CDCl_3$, δ) 5.63 (d, 2H, $^3J_{HH}$ = 6.0 Hz, C_6H_4), 5.51 (d, 2H, $^3J_{HH}$ = 6.0 Hz, C_6H_4), 4.37 (d, 6H, $^3J_{HP}$ = 5.0 Hz, $P(OCH_2)_3CCH_2CH_3$), 2.88 (sept, 1H, $^2J_{HH}$= 7 Hz, $(CH_3C_6H_4(CH)(CH_3)_2$), 2.16 (s, 3H, C_6H_4 CH_3), 1.32 1.15 (overlapping m s, 8H, coincidental overlap of $P(OCH_2)_3CCH_2CH_3$ and C_6H_4 $CH(CH_3)_2$), 0.84 (t, 3H, $^3J_{HH}$ = 8 Hz, $(P(OCH_2)_3CCH_2CH_3)$. ^{13}C NMR (75 MHz, $CDCl_3$) δ 108.9 (s, C_6H_4), 103.3 (s, C_6H_4), 90.1 (d, $^2J_{PC}$ = 7.1 Hz, C_6H_4), 89.3 (d, $^2J_{PC}$= 6.0 Hz, C_6H_4), 75.5 (d, $^2J_{CP}$ = 7.6 Hz, $P(OCH_2)_3CCH_2CH_3$), 36.1 ($^3J_{CP}$ = 32.2 Hz, $P(OCH_2)_3CCH_2CH_3$), 30.5 (s, C_6H_4-$CH(CH_3)_2$), 23.4 (s, $P(OCH_2)_3CCH_2CH_3$), 22.1 (s, C_6H_4-$(CH(CH_3)_2)$), 18.6 (s, C_6H_4-CH_3), 7.3 (s, $P(OCH_2)_3CCH_2CH_3$). ^{31}P{^{1}H} NMR (121 MHz, CD_2Cl_2, δ): 111.8 ($P(OCH_2)_2CEt$). HRMS: $[M + Na]^+$ obsd (%), calcd (%), ppm: 488.9858 (37.6), 488.98503 (32.9), 1.6; 489.98611 (62.9), 489.98504 (42), 2.2; 490.98525 (100), 490.98445 (100), 1.6; 491.98534 (44.5), 491.98404 (32.9), 2.6; 492.9845 (96.7), 492.98449 (94.8), 0; 493.98643 (85.5), 493.98554 (84.2), 1.8; 494.98312 (85.5), 494.98235 (84.2), 1.6. CV ($NCCH_3$): $E_{1/2}$ = 1.30 V Ru(III/II) (quasi-reversible); $E_{p,c}$ = 1.23 V Ru(II/I).

(η^6-p-cymene)Ru[P(OCH$_2$)$_2$(OCCH$_3$)]Cl$_2$ (13). A benzene solution of **1** (0.570 g, 4.25 mmol) was added to $[(\eta^6\text{-}p\text{-cymene})Ru(Cl)(\mu\text{-}Cl)]_2$ (0.369 g, 0.603 mmol) in CH_2Cl_2 (75 mL). The solution was stirred at room temperature for 30 min to give an orange solution. The solvent volume was reduced in vacuo to 25 mL. Hexanes were added to yield a red precipitate, which formed a red oil. The solution was filtered through Celite. The solid collected on Celite was eluted with CH_2Cl_2. The solvent was removed in vacuo. The resulting solid was washed with pentane. The solid was dried to yield a reddish-orange solid (0.489 g, 92.3%). This crude material was purified on an alumina column with 1:1 CH_2Cl_2/THF as eluent (0.088 mg, 20%). ^{1}H NMR (300 MHz, $CDCl_3$, δ) 5.76 (d, 2H, C_6H_4, $^3J_{HH}$ = 5.9 Hz), 5.62 (d, 2H, C_6H_4, $^3J_{HH}$ = 5.9 Hz), 4.22 (apparent t, 2H, $P(OCH_2)_2(OCCH_3)$, $^2J_{HH}$ = 8 Hz), 3.83 (d, 2H, $P(OCH_2)_2(OCCH_3)$ $^2J_{HH}$ = 7 Hz), 2.90 (sept, 1H, $(CH_3C_6H_4(CH)(CH_3)_2$ $^3J_{HH}$ = 7 Hz), 2.22 (s, 3H, C_6H_4 CH_3), 1.68 (s, 3H, $P(OCH_2)_2(OCCH_3)$), 1.23 (d, 6H, C_6H_4 $CH(CH_3)_2$, $^3J_{HH}$ = 7 Hz). ^{13}C NMR (75 MHz, $CDCl_3$, δ) 110.0 (s, C_6H_4), 106.2 (s, C_6H_4), 90.5 (C_6H_4), 90.4 (C_6H_4), 90.1 (C_6H_4), 90.1 (C_6H_4), 82.9 ($P(OCH_2)_2(OCCH_3)$), 75.7 (s, $P(OCH_2)_2(OCCH_3)$), 75.6 ($P(OCH_2)_2(OCCH_3)$), 30.9 (C_6H_4-$CH(CH_3)_2$), 22.3 (s, symm. equivalent C_6H_4 $C(CH_3)_2$), 18.8 (s, C_6H_4-CH_3), 15.3 (d, $^3J_{HH}$ = 10.4 Hz, $P(OCH_2)_2(OCCH_3)$). ^{31}P{^{1}H} NMR (121 MHz, $CDCl_3$ δ): 143.6 (s, $P(OCH_2)_2(OCCH_3)$). HRMS: $[M + Na]^+$ obsd (%), calcd (%), ppm: 460.95441 (37.4), 460.95328 (46.3), 2.5; 461.95477 (63), 461.95265 (60.9), 4.6; 462.95389 (100), 462.95262 (100), 2.7; 463.95387 (42.9), 463.95148 (48.6), 5.2; 464.95316 (97.1), 464.95168 (91.8), 3.2; 465.95496 (85.5), 465.95309 (84.2), 4; 466.95174 (85.5), 466.95034 (84.2), 3. CV ($NCCH_3$): $E_{1/2}$ = 1.44 V Ru(III/II) (quasi-reversible); $E_{p,c}$ = 1.05 V.

(η^6-p-cymene)Ru[P(OMe)$_3$]Cl$_2$ (14). The synthesis of complex **14** has been previously reported.[47] We used an alternate procedure, which is given below. $[(\eta^6\text{-}p\text{-cymene})Ru(Cl)(\mu\text{-}Cl)]_2$ (0.0517 g, 0.0844 mmol) was stirred at room temperature in CH_2Cl_2 (15 mL). $P(OMe)_3$ (0.0232 g, 0.187 mmol) was added by syringe. The solution was stirred at room temperature for 2 h after which time the solution was reduced in vacuo to 3 mL. Hexanes were added to yield an orange precipitate. The mixture was filtered through a fine porosity frit. The solid was washed with pentane and dried in vacuo to yield an orange solid (0.0553 g, 76.1% yield). ^{1}H NMR spectroscopy revealed clean material and was consistent with previously reported data.[47] CV ($NCCH_3$): $E_{1/2}$ = 1.25 V Ru(III/II) (quasi-reversible); $E_{p,c}$ = 1.21 V.

(η^6-p-cymene)Ru(PPh$_3$)Cl$_2$ (15). The synthesis of complex **15** has been previously reported.[47] We used an alternate procedure, which is given below. $[(\eta^6\text{-}p\text{-cymene})Ru(Cl)(\mu\text{-}Cl)]_2$ (0.400 g, 0.653 mmol) and PPh_3 (0.360 g, 1.37 mmol) were stirred at room temperature for 2 h in CH_2Cl_2 (15 mL), after which time the solution was reduced in vacuo to 3 mL. Hexanes were added to yield an orange precipitate. The mixture was filtered through a fine porosity frit. The solid was washed with pentane and dried in vacuo to yield an orange solid (0.658 g, 88.7% yield). ^{1}H NMR spectroscopy revealed clean material and was consistent with previously reported data.[47] CV ($NCCH_3$): $E_{1/2}$ = 1.25 V Ru(III/II); $E_{p,c}$ = 1.25 V.

General Procedure for the Measurement of Rates of Exchange. Stock solutions in $CDCl_3$ were prepared in a volumetric flask. Each kinetic experiment was performed in triplicate. For each experiment, $CDCl_3$ solutions of $P(OMe)_3$ and/or PPh_3 were combined in a screw cap NMR tube with $CDCl_3$ such that the reaction volume before addition of Ru complex totaled 0.40 mL. Immediately before placing the solution into the NMR probe (equilibrated at 58 C), 0.20 mL of the Ru complex (**12**, **13**, or **15**) (with hexamethyldisiloxane as an internal standard) was added by syringe to give a total volume 0.60 mL. The tube was inverted two times. Reaction progress was monitored by ^{1}H NMR spectroscopy using automated data acquisition. A single transient was used for each time point with 60 s delay between transients for reactions with solutions of **13** and **15**, and a 600 s between transients for reactions of complex **12**. The rate of the reaction was determined by monitoring the disappearance of starting material [complex **12**: 4.37 ppm [d, $^3J_{HP}$ = 5.0 Hz, $P(OCH_2)_3CCH_2CH_3$]; complex **15**: 1.87 ppm [s, (*p*-cymene) C_6H_4 CH_3], and complex **13**: 1.68 ppm [s, 3H, $P(OCH_2)_2(OCCH_3)$]. Each

dx.doi.org/10.1021/ic300109b | Inorg. Chem. 2012, 51, 4791 4801

reaction was monitored through at least 3.5 half-lives. Rates were determined by least-squares analyses of a plot of starting material vs time (seconds).

ASSOCIATED CONTENT

Supporting Information

Crystallographic data in CIF format. Further details are given in Figures S1 S9 and Tables S1 S3. This material is available free of charge via the Internet at http://pubs.acs.org.

AUTHOR INFORMATION

Corresponding Author

*E-mail: tbg7h@virginia.edu (T.B.G.).

Notes

The authors declare no competing financial interest.

ACKNOWLEDGMENTS

We acknowledge the Office of Basic Energy Sciences, U.S. Department of Energy, for support of this work [DE-SC0000776 (T.B.G.) and DE-FG02-03ER15387 (T.R.C.)] and the NSF (CHE-0320669) for financial support of instrumentation at the University of Richmond. We also thank Ms. Diana A. Iovan for assistance with acquisition of mass spec data.

REFERENCES

(1) Crabtree, R. H. *The Organometallic Chemistry of the Transition Metals*, 4th ed.; Wiley-Interscience: Hoboken, NJ, 2005; pp 99 103.

(2) Keiter, R. L.; Verkade, J. G. *Inorg. Chem.* **1970**, *9*, 404 406.

(3) Verkade, J. G.; McCarley, D. G.; Hendricker, D. G.; King, R. W. *Inorg. Chem.* **1965**, *4*, 228 231.

(4) Meiners, J. H.; Rix, C. J.; Clardy, J. C.; Verkade, J. G. *Inorg. Chem.* **1975**, *14*, 705 710.

(5) Serron, S.; Nolan, S. P.; Abramov, Y. A.; Brammer, L.; Petersen, J. L. *Organometallics* **1998**, *17*, 104 110.

(6) Tolman, C. A. *Chem. Rev.* **1977**, *77*, 313 348.

(7) Freixa, Z.; van Leeuwen, P. W. N. M. *Dalton Trans.* **2003**, 1890 1901.

(8) Bunten, K. A.; Chen, L.; Fernandez, A. L.; Poe, A. J. *Coord. Chem. Rev.* **2002**, *233 234*, 41 51.

(9) Leyssens, T.; Peeters, D.; Orpen, A. G.; Harvey, J. N. *Organometallics* **2007**, *26*, 2637 2645.

(10) Downing, J. H.; Smith, M. B. In *Comprehensive Coordination Chemistry II*; Elsevier: Amsterdam, The Netherlands, 2004; Vol. *1*, pp 253 296.

(11) Kuehl, O. *Coord. Chem. Rev.* **2005**, *249*, 693 704.

(12) Sasaki, S.; Yoshifuji, M. *Curr. Org. Chem.* **2007**, *11*, 17 31.

(13) van Leeuwen, P. W. N. M.; Freixa, Z.; Zuidema, E. *Phosphorus Ligands in Asymmetric Catalysis*; Wiley-VCH: Weinheim, Germany, 2008; Vol. *3*, pp 1433 1454.

(14) Muller, T. E.; Mingos, D. M. P. *Transition Met. Chem.* **1995**, *20*, 553 539.

(15) Gilheany, D. G. Structure and bonding in organophosphorus-(III) compounds. In *The Chemistry of Organophosphorus Compounds*; Hartley, F. R., Ed.; John Wiley & Sons: New York, 1990; Vol. *1*, pp 9 49.

(16) Valentine, D. H.; Hillhouse, J. H. *Synthesis* **2003**, 2437 2460.

(17) Meiners, J. H.; Clardy, J. C.; Verkade, J. G. *Inorg. Chem.* **1975**, *14*, 632 636.

(18) Hartwig, J. F. *Organotransition Metal Chemisty: from Bonding to Catalysis*. University Science Books: Herndon, VA, 2010; p 32 38.

(19) Valentine, D. H.; Hillhouse, J. H. *Synthesis* **2003**, 317 334.

(20) Kuehl, O. *Can. J. Chem.* **2007**, *85*, 230 238.

(21) Cao, M.; Do, L. V.; Hoffman, N. W.; Kwan, M. L.; Little, J. K.; McGilvray, J. M.; Morris, C. B.; Soderberg, B. C.; Wierzbicki, A.; Cundari, T. R.; Lake, C. H.; Valente, E. J. *Organometallics* **2001**, *20*, 2270 2279.

(22) Fortman, G. C.; Nolan, S. P. *Organometallics* **2010**, *29*, 4579 4583.

(23) Verkade, J. G.; Hutteman, T. J.; Fung, M. K.; King, R. W. *Inorg. Chem.* **1965**, *4*, 83 87.

(24) Heitsch, C. W.; Verkade, J. G. *Inorg. Chem.* **1962**, *1*, 392 398.

(25) Rix, C. J.; Verkade, J. G. *Coord. Chem. Rev.* **1975**, *16*, 129 139.

(26) Verkade, J. G. *Bioinorg. Chem.* **1974**, *3*, 165 182.

(27) Vande Griend, L. J.; Verkade, J. G.; Pennings, J. F. M.; Buck, H. M. *J. Am. Chem. Soc.* **1977**, *99*, 2459 2463.

(28) Verkade, J. G. *Coord. Chem. Rev.* **1972**, *9*, 1 106.

(29) Milbrath, D. S.; Springer, J. P.; Clardy, J. C.; Verkade, J. G. *J. Am. Chem. Soc.* **1976**, *98*, 5493 5496.

(30) Huttemann, T. J.; Foxman, B. M.; Sperati, C. R.; Verkade, J. G. *Inorg. Chem.* **1965**, 950.

(31) Foley, N. A.; Ke, Z. F.; Gunnoe, T. B.; Cundari, T. R.; Petersen, J. L. *Organometallics* **2008**, *27*, 3007 3017.

(32) Verkade, J. G.; Piper, T. S. *Inorg. Chem.* **1963**, *2*, 944 947.

(33) Denny, D. B.; Varga, S. L. *Phosphorus* **1973**, *2*, 245 248.

(34) Nifantyev, E. E.; Koroteev, A. M.; Koroteev, M. P.; Meshkov, S. V.; Belsky, V. K.; Bekker, A. R. *Phosphorus, Sulfur Silicon Relat. Elem.* **1996**, *113*, 1 13.

(35) Wadsworth, W. S.; Emmons, W. D. *J. Am. Chem. Soc.* **1962**, 610 617.

(36) Wirz, B.; Barner, R.; Hubscher, J. *J. Org. Chem.* **1993**, *58*, 3980 3984.

(37) Roebuck, A.; Adkins, H. A. *Organic Synthesis*; John Wiley & Sons, Inc.: New York, 1955; Vol. *3*.

(38) Slugovc, C.; Sapunov, V. N.; Wiede, P.; Mereiter, K.; Schmid, R.; Kirchner, K. *J. Chem. Soc., Dalton Trans.* **1997**, 4209 4216.

(39) Werner, H.; Brauers, G.; Nurnberg, O. *J. Organomet. Chem.* **1993**, *454*, 247 255.

(40) Zelonka, R. A.; Baird, M. C. *Can. J. Chem.* **1972**, *50*, 3063 3072.

(41) Bennett, M. A.; Smith, A. K. *J. Chem. Soc., Dalton Trans.* **1974**, 233 241.

(42) Werner, H.; Werner, R. *Chem. Ber.-Recl.* **1982**, *115*, 3766 3780.

(43) Zelonka, R. A.; Baird, M. C. *J. Organomet. Chem.* **1972**, *35*, C43 C46.

(44) Elsegood, M. R. J.; Tocher, D. A. *Polyhedron* **1995**, *14*, 3147 3156.

(45) Pigge, F. C.; Coniglio, J. J. *Curr. Org. Chem.* **2001**, *5*, 757 784.

(46) Bard, A. J.; Faulkner, L. R. *Electrochemical Methods: Fundamentals and Applications*, 2nd ed.; John Wiley & Sons: New York, 2001; p 231.

(47) Hodson, E.; Simpson, S. J. *Polyhedron* **2004**, *23*, 2695 2707.

(48) Furstner, A.; Liebl, M.; Lehmann, C. W.; Picquet, M.; Kunz, R.; Bruneau, C.; Touchard, D.; Dixneuf, P. H. *Chem. Eur. J.* **2000**, *6*, 1847 1857.

(49) Elsegood, M. R. J.; Smith, M. B.; Sanchez-Ballester, N. M. *Acta Crystallogr., Sect. E* **2006**, *62*, M2838 M2840.

(50) Orpen, A. G.; Connelly, N. G. *J. Chem. Soc., Chem. Commun.* **1985**, 1310 1311.

(51) Dias, P. B.; Depiedade, M. E. M.; Simoes, J. A. M. *Coord. Chem. Rev.* **1994**, *135*, 737 807.

(52) Jover, J.; Fey, N.; Harvey, J. N.; Lloyd-Jones, G. C.; Orpen, A. G.; Owen-Smith, G. J. J.; Murray, P.; Hose, D. R. J.; Osborne, R.; Purdie, M. *Organometallics* **2010**, *29*, 6245 6258.

(53) Ellis, D. D.; Haddow, M. F.; Orpen, A. G.; Watson, P. J. *Dalton Trans.* **2009**, 10436 10445.

(54) Taira, K.; Mock, W. L.; Gorenstein, D. G. *J. Am. Chem. Soc.* **1984**, *106*, 7831 7835.

(55) Belyakov, A. V.; Dalhus, B.; Haaland, A.; Shorokhov, D. J.; Volden, H. V. *J. Chem. Soc., Dalton Trans.* **2002**, 3756 3762.

(56) Slater, J. C. *Quantum Theory of Molecules and Solids*; McGraw-Hill: New York, 1974; Vol. *4*, The Self-Consistent Field for Molecules and Solids.

(57) Becke, A. D. *Phys. Rev. A* **1988**, *38*, 3098 3100.

(58) Perdew, J. P. *Phys. Rev. B* **1986**, *34*, 7406 7406.

(59) Perdew, J. P. *Phys. Rev. B* **1986**, *33*, 8822 8824.
(60) Perdew, J. P.; Zunger, A. *Phys. Rev. B* **1981**, *23*, 5048 5079.
(61) Hay, P. J.; Wadt, W. R. *J. Chem. Phys.* **1985**, *82*, 270 283.
(62) Pyykko, P.; Mendizabal, F. *Inorg. Chem.* **1998**, *37*, 3018 3025.
(63) Couty, M.; Hall, M. B. *J. Comput. Chem.* **1996**, *17*, 1359 1370.
(64) Frisch, M.J.; Trucks, G. W.; Schlegel, H. B.; Scuseria, G. E.; Robb, M. A.; Cheeseman, J. R.; Scalmani, G.; Barone, B. M.; Petersson, G. A.; Nakatsuji, H.; Caricato, M.; Li, X.; Hratchian, H. P.; Izmaylov, A. F.; Bloino, J.; Zheng, G.; Sonnenberg, J. L.; Hada, M.; Ehara, M.; Toyota, K.; Fukuda, R.; Hasegawa, J.; Ishida, T. N.; Honda, Y.; Kitao, O.; Nakai, H.; Vreven, T.; Montgomery, J.A.; Jr.; Peralta, J. E.; Ogliaro, M. B.; Heyd, J. J.; Brothers, E.; Kudin, K. N.; Staroverov, V. N.; Kobayashi, R.; Normand, K. R.; Rendell, A.; Burant, J. C.; Iyengar, S. S.; Tomasi, J.; Cossi, M.; Rega, N.; Millam, J. M.; Knox, J. E.; Cross, J. B.; Bakken, V.; Adamo, C.; Jaramillo, J.; Gomperts, R.; Stratmann, R. E.; Austin, A. J.; Cammi, R.; Pomelli, C.; Ochterski, J. W.; Martin, R. L.; Morokuma, K.; Zakrzewski, V. G.; Voth, G.; Salvador, P.; Dannenberg, J. J.; Dapprich, S.; Daniels, A.D.; Farkas, O.; Foresman, J. B.; Cioslowski, J.; Fox., D. J. *Gaussian 09*, Revision A.1; Gaussian, Inc.: Wallingford, CT, 2009.